THE AMERICAN SOCIETY OF MECHANICAL ENGINEERS
345 E. 47 St., New York, N.Y. 10017

84-APM-18

On the Propagation of Bulges and Buckles[1]

E. Chater

J. W. Hutchinson
Mem. ASME

Division of Applied Sciences,
Harvard University,
Cambridge, Mass. 02138

Two examples illustrate the propagation of instability modes under quasi-static, steady-state conditions. The first is the inflation of a long cylindrical party balloon in which a bulge propagates down the length of the balloon. The second is the collapse of a long pipe under external pressure as a result of buckle propagation. In each example, there is a substantial barrier to the initiation of the instability mode. Once initiated, however, the mode will not arrest if the pressure is in excess of the quasi-static, steady-state propagation pressure. It is this critical pressure that is determined in this paper for each of the two examples.

1 Introduction

While not a problem of great technological importance, the inflation of a common cylindrical party balloon provides a good illustration of the phenomenon of the propagation of an instability. If one were to record the pressure in the balloon as a function of its volume during the inflation process, one would obtain a record such as that shown in Fig. 1. A bulge first starts to form when the peak pressure is attained. It forms and localizes at some section with an initial weakness or at one of the ends of the balloon due to local nonuniformity. With continued inflation, the pressure falls to a constant level as the bulge slowly propagates along the balloon. During the steady-state portion of the inflation process the radii of the bulged and unbulged sections do not change, as depicted in Fig. 1. The transition front between these two sections simply propagates, or translates, into the unbulged section. This is a quasi-static process in that air mass (essentially volume), and not pressure, is prescribed to increase at a slow rate. A photograph of a partially inflated cylindrical balloon in the steady-state phase of the inflation process is shown in Fig. 2. Our analysis will focus on the critical pressure p^* associated with quasi-static, steady-state bulge propagation and on the states on either side of the transition.

The balloon problem is analogous in several respects to the second problem we will consider, which is the collapse of a long cylindrical shell, or pipe, due to the propagation of a buckle along its length. This problem is of some importance in connection with the collapse of undersea pipelines. We address the problem of the external pressure p^* required to propagate a buckle down the pipe under steady, quasi-static conditions. This critical pressure is especially significant since at any pressure below p^*, buckles cannot propagate, while at any prescribed pressure above p^*, the buckle once initiated will run dynamically, collapsing the entire length of pipe.

2 Steady-State Bulge Propagation Along a Cylindrical Balloon

To gain a qualitative understanding of the origin of the initial bulging process and the subsequent quasi-static bulge propagation along a cylindrical party balloon, one need only consider the relation of pressure to change of volume for a cylindrical section of the balloon. Consider purely cylindrical membrane deformations of a section such that at any pressure p the shape is always cylindrical with current radius R and thickness t. The circumferential stress is $\sigma_2 = pR/t$ and the axial stress is $\sigma_1 = pR/(2t)$. The qualitative form of the curve of pressure as a function of volume for a cylindrical section of balloon that has unit volume in the undeformed state is shown in Fig. 3. The volume change results from axial as well as circumferential stretch. It will be assumed that the balloon is inflated under isothermal conditions, and that the pressure-volume relation in Fig. 3 for purely cylindrical deformations corresponds to isothermal deformation of the balloon rubber. A curve calculated using a constitutive law for an actual rubber will be displayed later.

The initial bulging is a consequence of the local peak in the curve of pressure against volume for purely cylindrical deformations. The qualitative argument for initial bulge formation parallels that of Considére for necking of metal bars in tension. One section, which is slightly weaker than the rest of the balloon, attains the peak first and then bulges under falling pressure while the remainder of the balloon "unloads" without bulging. The bulge has localized in the manner described in general terms by Tvergaard and Needleman [1]. However, unlike tensile necking in common metals and many other problems involving localized instability modes, the bulge starts to spread as inflation is continued. Spreading, or propagation, is associated with the upturn in the curve of pressure versus volume for the cylindrical section. The increasing resistance of a bulged section to

Contributed by the Applied Mechanics Division for presentation at the 1984 PVP Conference and Exhibition, Joint with Applied Mechanics Division and Materisls Division, San Antonio, Texas, June 17-21, 1984 of THE AMERICAN SOCIETY OF MECHANICAL ENGINEERS.

Discussion on this paper should be addressed to the Editorial Department, ASME, United Engineering Center, 345 East 47th Street, New York, N.Y. 10017 and will be accepted until two months after final publication of the paper itself in the JOURNAL OF APPLIED MECHANICS. Manuscript received by ASME Applied Mechanics Division, June, 1983. Paper No. 84-APM-18.

Copies will be available until February, 1985.

[1] Dedicated to the memory of B. O. Almroth.

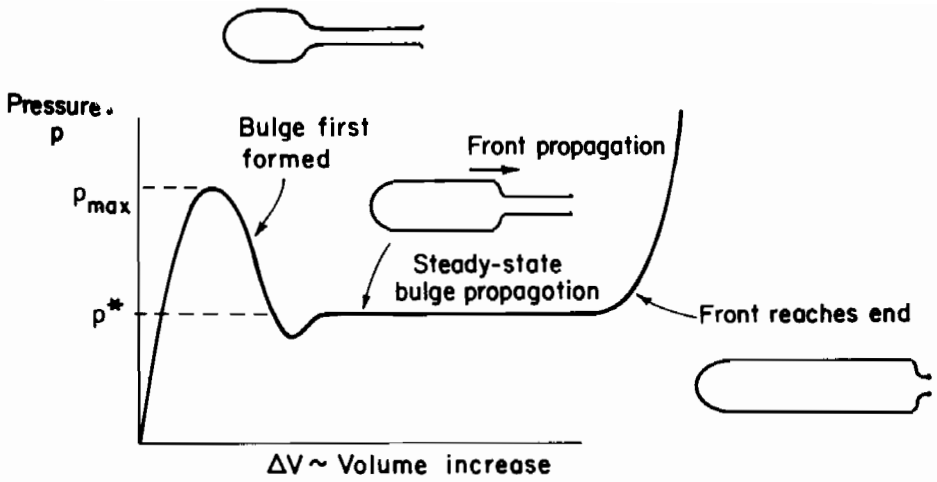

Fig. 1 Inflation of a cylindrical party balloon

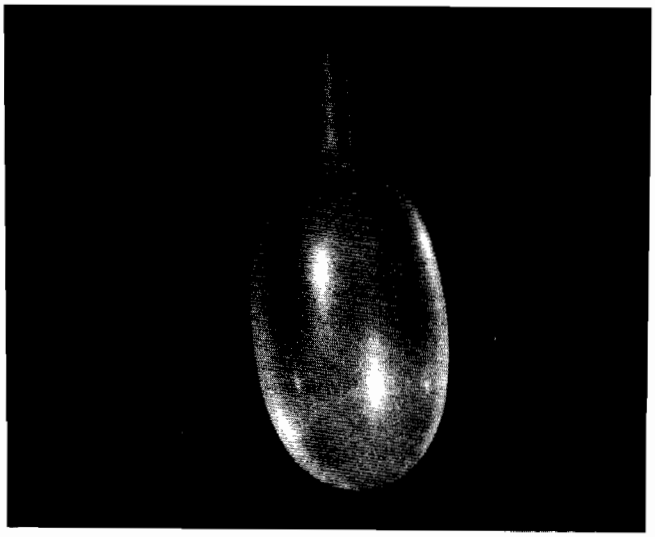

Fig. 2 Common party balloon showing transition between bulged and unbulged sections

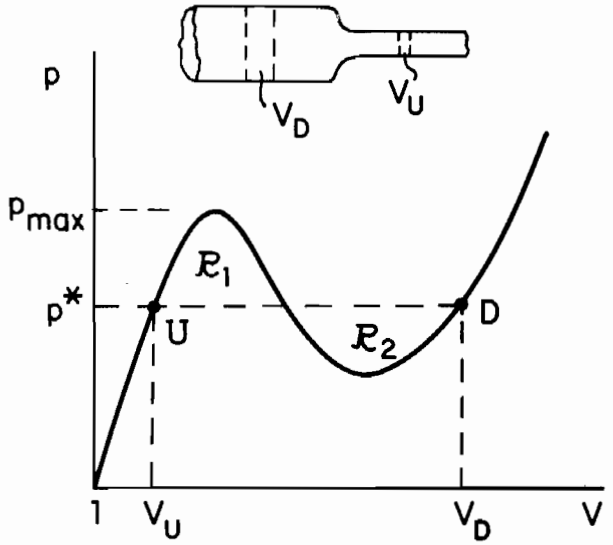

Fig. 3 $p(V)$ for purely cylindrical deformation of a cylindrical segment of unit initial volume. Quasi-static, steady-state propagation condition requires $\mathcal{R}_1 = \mathcal{R}_2$.

further volume expansion terminates the localization process and forces the bulge to propagate laterally into the neighboring section.

Condition for Steady-State Propagation. As discussed in the Introduction and as depicted in Fig. 1, the inflation process soon reaches a steady state in which the pressure is constant and the radii of the bulged and unbulged sections do not change. The transition front between these two sections attains a fixed shape which simply translates along the balloon engulfing the unbulged section. We will be concerned with steady-state inflation under a sufficiently slow rate of air injection such that inertial effects are negligible. This is quasi-static bulge propagation in which the advance of the transition front is controlled by the rate of air injection. Depending on the properties of the balloon material and on its length, the initial bulging process may occur dynamically, under a prescribed mass of air, with the bulging section growing at the expense of the remainder of the balloon.

The equation determining the quasi-static propagation pressure p^* under steady-state conditions follows immediately from the energy balance requirement that the work done by p^* must equal the change of strain energy stored in the balloon in any advance of the transition front.

Let V_U and V_D denote the volumes of cylindrical sections, each with unit undeformed volume, associated with states U and D far ahead of and far behind, respectively, the transition. Because the shape of the transition is fixed, the change in volume of the balloon when the transition front shifts forward to engulf a new section that has unit undeformed volume is precisely $V_D - V_U$, and the work done by the pressure is $p^*(V_D - V_U)$. This work of the pressure is equal to the work, ΔW, done on a section of unit undeformed volume as it passes from state U to state D through the transition, i.e.,

$$p^*(V_D - V_U) = \Delta W \tag{1}$$

Now, for a rubberlike material for which a strain energy function is assumed to exist (under the assumed isothermal conditions), ΔW is independent of the details of the deformation history in the transition and depends only on the end states D and U. In particular, we may calculate ΔW using purely cylindrical deformations to connect states D and U. Doing so, we note that

$$\Delta W = \int_{V_U}^{V_D} p(V)\,dV \tag{2}$$

where $p(V)$ denotes the relation of pressure to volume for purely cylindrical deformations of a section of unit undeformed volume, such as that depicted in Fig. 3. Thus, from (1) and (2), the equation for the pressure p^* for quasi-static, steady-state bulge propagation is

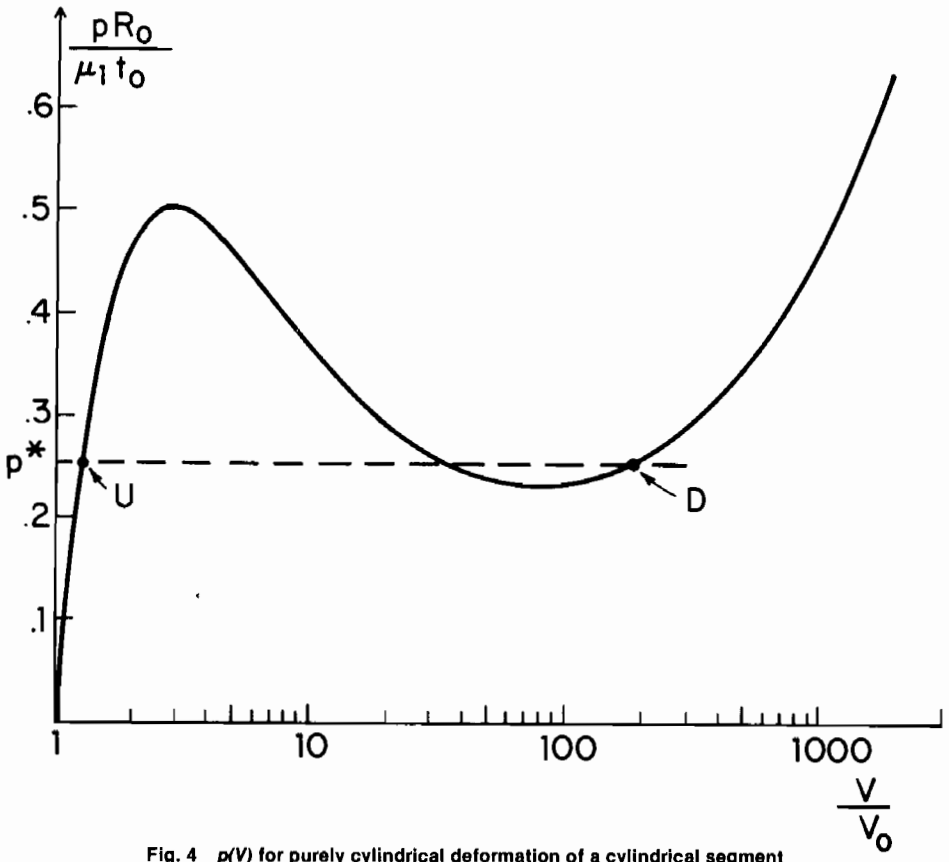

Fig. 4 *p(V)* **for purely cylindrical deformation of a cylindrical segment of rubber material specified by (4)–(6). (The logarithmic scale distorts the areas of the two lobes.)**

$$p^*(V_D - V_U) = \int_{V_U}^{V_D} p(V)\,dV \tag{3}$$

Equation (3) has the simple graphical solution indicated in Fig. 3. By (3), the equality of the rectangular area $p^*(V_D - V_U)$ with the area under the curve $p(V)$ between V_U and V_D is equivalent to the condition that the areas of the two lobes, $\mathfrak{R}_1$ and $\mathfrak{R}_2$, be equal. In the literature of phase transitions, this graphical solution involving conjugate thermodynamical variables is known as Maxwell's condition for two coexisting phases [2]. For the balloon, equation (3) is the condition that a transition between bulged and unbulged sections exist whether the transition is stationary or whether it is propagating quasi-statically under inflation or deflation.

The quasi-static propagation pressure p^* is less than the local peak pressure $p_{\max}$ a cylindrical segment can support by about a factor of two, which will be shown in the following example. In other words, it takes a substantially larger pressure to initiate a bulge than to propagate it, as depicted in Fig. 1, and as experienced by anyone familiar with blowing up party balloons. The relevance of the Maxwell construction to other instability propagation problems has been noted in [3, 4]. Characteristic of the general class of phenomena is a substantial barrier to the initiation of the instability mode. Once initiated, the mode encounters less resistance and spreads at reduced load.

Predictions for a Specific Rubber Material. Ogden [5] proposed a strain energy density function for incompressible, isotropic rubberlike materials in the form

$$\Phi = \sum_{i=1}^{3} \mu_i I(\alpha_i) \tag{4}$$

where

$$I(\alpha) = \alpha^{-1}(\lambda_1^\alpha + \lambda_2^\alpha + \lambda_3^\alpha - 3) \tag{5}$$

and where the λ_i are the three stretches. To fit Treloar's isothermal data for rubber, Ogden proposed

$$\alpha_1 = 1.3, \quad \alpha_2 = 5.0, \quad \alpha_3 = -2.0$$

with (6)

$$\mu_2 = 2.01 \times 10^{-3}\mu_1 \quad \text{and} \quad \mu_3 = -1.59 \times 10^{-2}\mu_1$$

where μ_1 is a ground state modulus which will not have to be specified here. The curve of nondimensional p as a function of V for purely cylindrical deformations of a cylindrical segment of this material is shown in Fig. 4. Here R_0, t_0, and V_0 denote the values of the radius, thickness, and volume of the undeformed cylindrical segment. The local peak pressure is

$$p_{\max} = 0.504\mu_1 t_0/R_0 \tag{7}$$

The Maxwell condition (3) for p^* and states U and D gives

$$p^* = 0.255\mu_1 t_0/R_0 \tag{8}$$

and

$$\begin{aligned} &\lambda_1^U = 1.006, \quad \lambda_2^U = 1.125, \quad V_U = 1.273V_0 \\ &\lambda_1^D = 4.484, \quad \lambda_2^D = 6.507, \quad V_D = 189.8V_0 \end{aligned} \tag{9}$$

where the one-direction is parallel to the cylindrical axis of the balloon and the two-direction is along its circumference. (Note that a logarithmic scale is used for the abscissa in Fig. 4 so that the two lobes formed by the Maxwell line do not have equal areas in that plot.) The steady-state inflation pressure is almost exactly one half $p_{\max}$. The measured volume expansion of the balloon of Fig. 2 in state D is about $V_D \cong 130V_0$, which is somewhat less than the prediction (9) for a balloon of Treloar's rubber characterized by (4).

Fig. 5 Section of one of Kyriakides' specimens showing the transition between the buckled and unbuckled regions of the pipe.

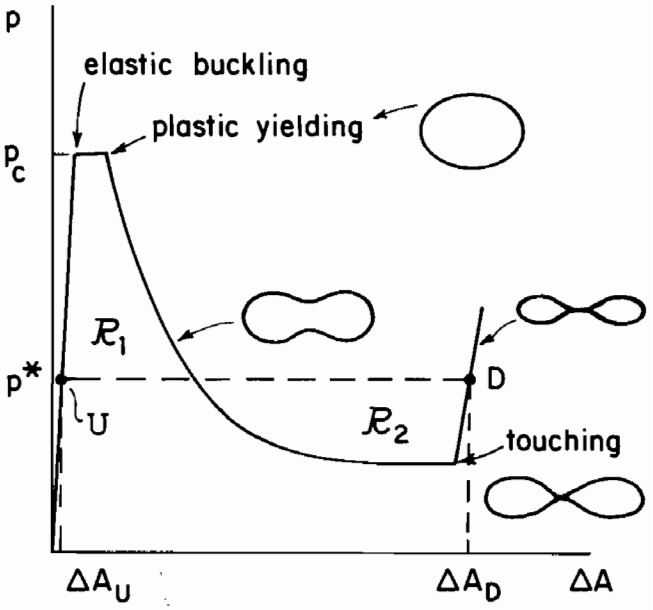

Fig. 6 Buckling and post-buckling behavior of a ring undergoing plane strain deformation. Quasi-static propagation pressure p^* is given by the condition $\mathcal{R}_1 = \mathcal{R}_2$ for a pipe of material characterized by deformation theory.

3 Buckle Propagation Along a Pipe Subject to External Pressure

We now direct attention to the problem for the smallest pressure at which a buckle, once initiated, will propagate the entire length of a cylindrical shell or pipe. Palmer and Martin [6] have given one of the early accounts of this phenomenon as related to the collapse of undersea pipelines, and Mesloh, Johns, and Sorenson [7] conducted the first systematic experimental study of the problem using both small and full-scale specimens. Kyriakides [8] and Kyriakides and Babcock [9, 10] have carried out the most extensive theoretical and experimental study of a number of aspects of buckle propagation and arrest on externally pressurized pipes. The approach we discuss in the following makes close contact with the work of Kyriakides and Babcock and, in particular, we will compare our theoretical predictions for the smallest propagation pressure to some of their experimental results.

A photograph of one of Kyriakides' test specimens is shown in Fig. 5. The section of pipe shown was cut from a much longer pipe. It displays the three regions of interest: the collapsed region, the unbuckled region, and the transition. In conducting the test, a substantial dent was introduced near one end of the long pipe. The pipe was then subjected to external pressure in an apparatus consisting of an external shell surrounding the pipe. Air or water was pumped at a given rate into the cavity between the pipe and the outer shell. Under quasi-static propagation of interest here, the buckle spreads at a rate that is controlled by the (slow) rate of injection of the pressurizing medium. After a brief transient, the propagating buckle settles down to a steady-state condition in which the transition moves down the pipe under constant pressure p^* leaving a plastically collapsed pipe behind it.

Buckling and Post-Buckling Behavior of a Ring Under Plane Strain Deformations. The classical elastic buckling pressure of an infinitely long cylndrical shell of radius R and thickness t due to plane strain ring buckling is

$$p_c = \frac{E}{4(1-\nu^2)}\left(\frac{t}{R}\right)^3 \tag{10}$$

where E is Young's modulus and ν is Poisson's ratio. The associated hoop stress in the shell at buckling is $\sigma_c = -p_c R/t$ and the axial stress is $\sigma_c/2$. The pipes that have been tested have ratios of radius to thickness in the range from about 15–50, roughly corresponding to the range of interest for undersea pipelines. In this range, the materials of the test specimens, and of the pipelines themselves, have sufficiently high-yield stresses such that any perfect pipe would begin to buckle elastically. That is, the stress state $(\sigma_c, \sigma_c/2)$ falls within the initial yield surface of the pipe material. In the present study, we will also confine attention to the range of parameters such that the classical buckling stress of the perfect pipe is within the elastic limit.

Kyriakides and Babcock [8–10] and Kyriakides and Arikan [11] have emphasized the relevance of the post-buckling behavior of a circular ring to the understanding of the buckle propagation problem, and the ring behavior is central to our approach as well. A schematic curve of pressure, p, as a function of reduction in cross-sectional area, ΔA, is shown in Fig. 6 for a perfect, infinitely long cylindrical shell undergoing ring buckling. This is a plane-strain ring mode in that the deformation is independent of the axial coordinate and the axial component of strain associated with bending is zero.

Buckling starts when the pressure attains p_c, as already described. Ovalization proceeds under a very slight rise in pressure until plastic yielding starts at the regions of highest curvature change. Once yielding starts, the pressure carrying capacity falls precipitously. As ovalization progresses, most of the deformation becomes confined to four "hinges" at the quarter points of the ring and the pressure falls more slowly. Then, when the area reduction has reached about 75 percent of the original cross-sectional area, touching of two opposite quarter points occurs, as depicted in Fig. 6. Touching braces the ring and immediately results in a substantial stiffening so that the pressure again increases very rapidly with relatively little additional area reduction [11].

Touching and the attendant rise in pressure is crucial to the work balance relation, and therefore some further

background to its occurrence is now given. In the original tests of Kyriakides and Babcock the importance of touching, per se, was not obvious and no effort was made to ascertain whether or not it occurred in the limit of quasi-static propagation. In the unloaded state the opposite walls of the collapsed section are definitely not in contact, but no conclusion can be drawn from this observation since elastic spring back always occurs. We are grateful to Kyriakides for conducting further tests on two additional specimens under quasi-static test conditions. In these tests he determined unambiguously that touching does occur in the collapsed section of the pipe behind the transition (private communication).

Deformation Theory Analysis of Quasi-Static, Steady-State Buckle Propagation. A second crucial aspect in our approach is the idealized material model we adopt. We characterize the material by the deformation theory of plasticity, which is a small-strain, nonlinearly elastic constitutive relation. In the steady-state buckle propagation problem elastic unloading is not an important feature. Almost every material point in the pipe experiences a monotonic plastic loading history as the transition fronts sweeps by it. In the quasi-static propagation limit, the transition between the collapsed and uncollapsed sections of the pipe is very gradually occurring over about 10 pipe diameters [8]. To a rough approximation, any short cylindrical segment of the pipe experiences a deformation history similar to the ring deformation depicted in Fig. 6. In addition to circumferential bending associated with the ring deformation, some axial bending along with in-plane straining must occur in the transition. In other words, although the stress history of any material point may involve monotonic loading, it is not a strictly proportional stressing history. By invoking deformation theory, we will be neglecting any path-dependent effects associated with the nonproportional stressing that occurs in the transition.

Now consider the work balance for steady-state propagation under quasi-static conditions at pressure p^*. By making the same simple arguments used in the balloon problem, one arrives at the work balance relation

$$p^*(\Delta A_D - \Delta A_U) = \Delta W \tag{11}$$

Here, ΔA_D and ΔA_U denote area reductions associated with segments far behind and far ahead of the transition, and ΔW is the stress work absorbed by each ring segment of unit length as it is engulfed by the transition deforming it from state U to state D. For a pipe of deformation theory material, states D and U are plane-strain ring solutions. Furthermore, because of the path independence of deformation theory, ΔW may be determined using the ring solution even though each ring segment departs from the plane-strain ring behavior in the transition. The stress work difference, ΔW, is just the work done on the plane strain ring in deforming it from state U to state D, i.e.,

$$\Delta W = \int_{\Delta A_U}^{\Delta A_D} p(\Delta A)\, d\Delta A \tag{12}$$

where $p(\Delta A)$ denotes the relation of pressure to area reduction for the ring under plane strain deformations. Thus, the equation for p^* is

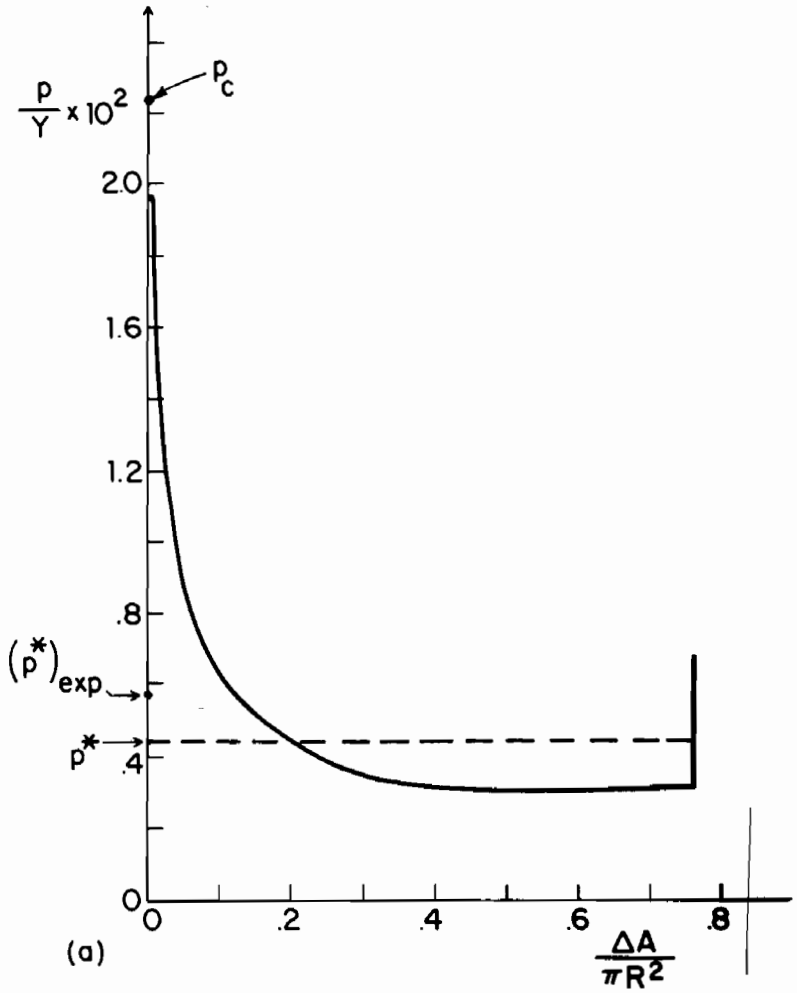

Fig. 7(a) $R/t = 14.3$

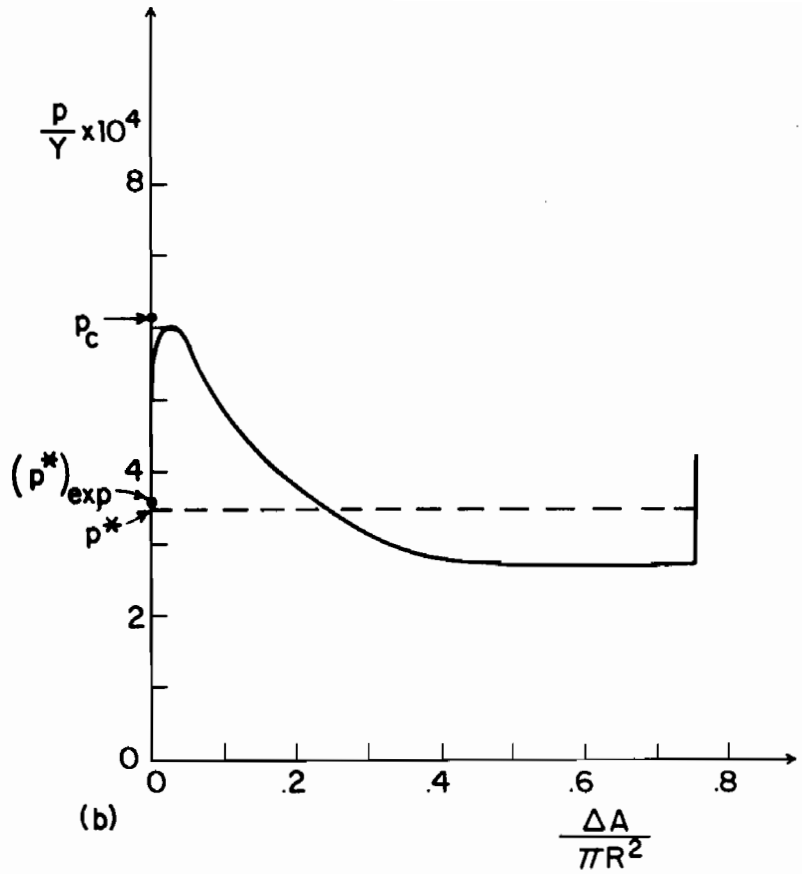

Fig. 7(b) $R/t = 47.4$

Fig. 7 Curves of $p(\Delta A)$ for cylindrical segments of two pipes in the test series. In each case, $Y/E = 0.0042$ and $n = 30$.

$$p^*(\Delta A_D - \Delta A_U) = \int_{\Delta A_U}^{\Delta A_D} p(\Delta A)\, d\Delta A \tag{13}$$

with the same graphical interpretation as in the balloon problem, as indicated in Fig. 6.

Comparison With Some Experiments. We have carried out accurate calculations of p^* for some pipes of AL-6061-T6 for which Kyriakides [8] reported quasi-static buckle propagation pressures. The yield stresses of the pipes in the test series ranged from $Y = 280$ to 370 MPa. We selected eight pipes for which the uniaxial stress-strain curves were available with Y being in the range from 286 to 296 MPa. The uniaxial curves given in [8] were closely approximated by the formula

$$\epsilon = \frac{\sigma}{E} + \left(0.005 - \frac{Y}{E}\right)\left(\frac{\sigma}{Y}\right)^n \tag{14}$$

where $E = 6.9 \times 10^4$ MPa, with $Y/E = 0.0042$ and $n = 30$ or with $Y/E = 0.0043$ and $n = 28$.

The pipes varied in radius to thickness from 14.3–47.4 and, as already mentioned, a perfect version of each would begin buckling in the elastic range. Some of the details of the calculation of the relation $p(\Delta A)$ for the plane-strain ring problem are described in the Appendix. Two examples are shown in Fig. 7 for the pipes in the series with the largest and smallest values of R/t. The elastic contraction of the ring prior to buckling is so small that almost no reduction of area shows up in Fig. 7 before the peak is attained. To facilitate the numerical calculation of $p(\Delta A)$, a very small initial imperfection was introduced in the form of an initial ovalization of the ring amounting to an additional radius difference of 0.005 times the ring thickness. For this reason, the peak value

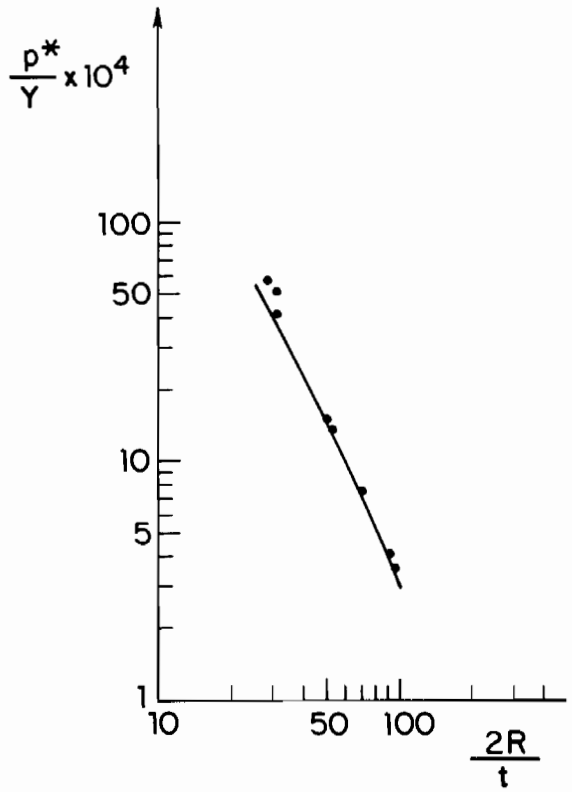

Fig. 8 Comparison of theoretical prediction for p^* (solid line) with experimental results of [8] (solid points)

Table 1

R(mm)	t(mm)	R/t	(experimental) p^*(MPa)	(theoretical) p^*(MPa)	Y(MPa)
12.7	0.889	14.3	1.68	1.29[a]	290
19.1	1.245	15.3	1.55	1.15[b]	297
14.3	0.914	15.6	1.23	1.11[b]	297
12.7	0.509	25.0	0.441	0.431[a]	290
19.1	0.737	25.9	0.395	0.394[a]	290
17.5	0.508	34.4	0.227	0.207[b]	297
25.4	0.559	45.5	0.121	0.110[b]	293
34.9	0.737	47.4	0.103	0.101[a]	286

[a] Calculated with $Y/E = 0.0042$ and $n = 30$
[b] Calculated with $Y/E = 0.0043$ and $n = 28$

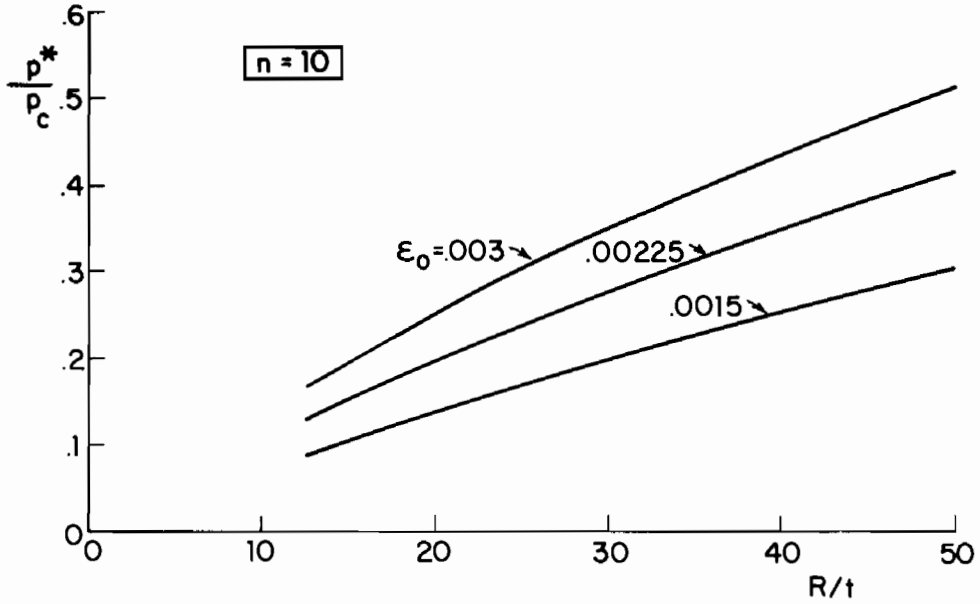

Fig. 9 p^*/p_c for various initial yield strains ϵ_0 for $n = 10$.

of p does not quite attain p_c. The error in p^* associated with the introduction of the imperfection is very small, as can readily be estimated.

Touching occurs at $\Delta A \cong 0.75\pi R^2$. We did not compute $p(\Delta A)$ beyond touching. For simplicity, we took the relation to have a vertical slope once touching occurred. This neglects a small contribution to the area of the lobe below the Maxwell line. The theoretical prediction for p^* determined from (13) is shown in each of the plots of Fig. 7 along with the experimental value.

The comparison between theory and experimental data for the eight pipes is graphed in Fig. 8. The theoretical curve in this figure was determined using $Y/E = 0.0042$ and $n = 30$, but essentially identical results are obtained using $Y/E = 0.0043$ and $n = 28$. Numerical data for the eight shells are given in Table 1. Except for the two pipes with the smallest values of R/t, the theoretical prediction for p^* underestimated the experimental propagation pressure by no more than 10 percent, and for three of the pipes the prediction is within 2 percent. The theoretical predictions for the two pipes with the smallest values of R/t underestimate the experimental propagation pressures by about 25 percent.

The results of a limited parameter study are presented in Figs. 9 and 10 in the form of curves of p^*/p_c versus R/t for various values of ϵ_0 and n. The uniaxial stress-strain curve in each case was the Ramberg-Osgood relation

$$\epsilon/\epsilon_0 = \sigma/\sigma_0 + (3/7)(\sigma/\sigma_0)^n \tag{15}$$

where $\epsilon_0 = \sigma_0/E$. The predictions for p^* are more sensitive than one might first suppose to the parameters characterizing the uniaxial stress-strain curve. For this reason, we have not attempted to make further comparisons with additional experimental results in [8] since detailed uniaxial material data were not available for the other test specimens. In this connection, it is almost certainly the uniaxial data associated with the circumferential direction that is relevant when the pipe material displays appreciable anisotropy.

It can be noted in Figs. 9 and 10 that the pipes with the smallest values of R/t have the smallest ratios of p^* to p_c. Buckle propagation pressures as low as 1/10 to 1/4 of the classical ring buckling pressure (10) are seen for pipes with R/t values in the range from 15–20. Such low buckle propagation pressures are surprising in light of the fact that the long cylindrical shell under external pressure is not normally regarded as very imperfection-sensitive even when plastic yielding occurs in the post-buckling response. It does take a substantial dent or blow to initiate a buckle that will then propagate. A pipe meeting normal tolerances should have no difficulty supporting pressures that are several times p^* as long as they are below p_c. However, if substantial dents or blows are possible, the pressure must be below p^* if it is to be certain that collapse of a full length of pipe will not occur. The spreading of a buckle due to an initial imperfection is studied in more detail for a model problem in [3].

Limitations of the Method. There is no question that deformation theory gives an oversimplified description of the pipe material for the buckle propagation problem. That the deformation theory predictions for p^* do so well, particularly for the pipes with the larger values of R/t, is probably a consequence of the gradual transition so that the departure from plane-strain ring behavior is not too marked. In every

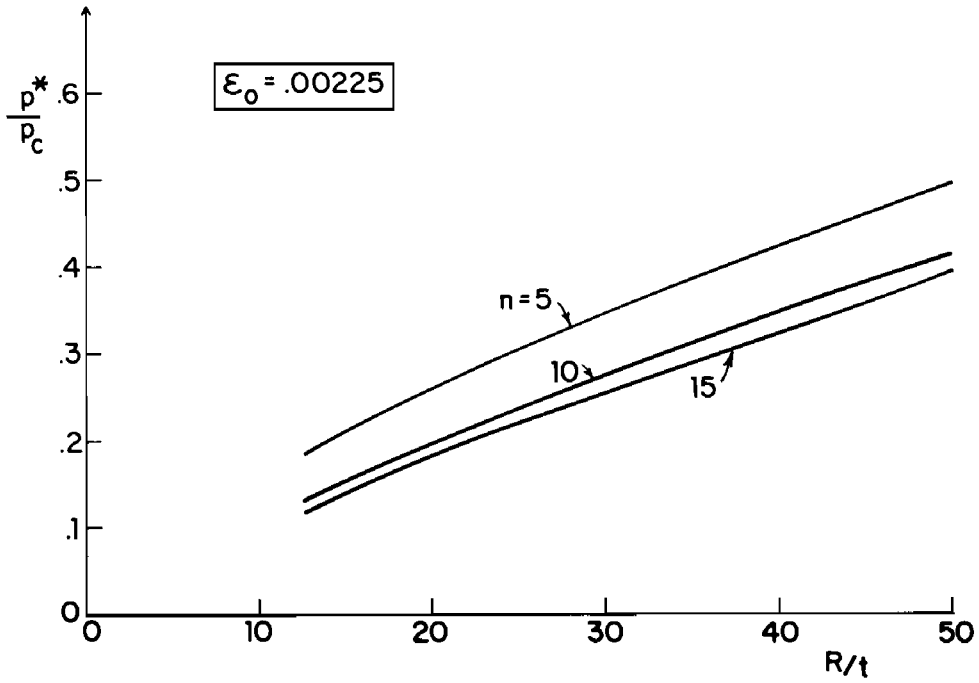

Fig. 10 p^*/p_c for various strain hardening exponents n for $\epsilon_0 = 0.00225$.

case, the deformation theory prediction for p^* underestimated the experimental result. This is not surprising since deformation theory is expected to underestimate the work absorbed, ΔW, by each ring segment as it is engulfed by the transition.

The simple analysis presented here provides the propagation pressure p^* and the states far ahead and behind the transition but no information about the transition itself. In the case of the balloon, we have formulated and solved the axisymmetric membrane problem for the full problem, including the transition, and this solution will be reported elsewhere, along with some results related to the energy associated with the transition. The corresponding problem for the pipe is much harder even when deformation theory is invoked.

We have made some attempts to base the calculation of p^* on an incremental theory of plasticity, but only with limited success at this stage. When deformation theory is abandoned and material path dependence is accounted for, the behavior in the transition must be analyzed. The appropriate shell problem is incomparably more difficult than the ring problem on which the deformation theory analysis is based. Nevertheless, at some level of approximation, it will probably be necessary to incorporate the effect of the material path dependence to improve on the present method for estimating p^*. Furthermore, if it is desired to predict the relation between the steady-state velocity of propagation at pressures above p^*, it will almost certainly be necessary to improve on the material model. As reported in [8], the transition is sharper in the dynamic problem than it is in the quasi-static one, and this makes it more likely that path-dependent effects are important in the transition.

Acknowledgment

C. D. Babcock, A. C. Palmer, and S. Kyriakides each helped to inform us about the buckle propagation problem. We are particularly indebted to S. Kyriakides for conducting the additional tests determining whether or not the opposite walls of the collapsed pipe come into contact under quasi-static propagation conditions. The work of E. C. was supported in part by the Natural Sciences and Engineering Research Council of Canada and by the National Science Foundation under Grant MEA-82-13925. The work of J. W. H. was supported in part by the National Science Foundation under Grant MEA-82-13925 and by the Division of Applied Sciences, Harvard University.

References

1 Tvergaard, V., and Needleman, A., "On the Localization of Buckling Patterns," ASME JOURNAL OF APPLIED MECHANICS, Vol. 47, 1980, pp. 613-619.

2 James, R. D., "Co-Existent Phases in the One-Dimensional Static Theory of Elastic Bars," *Archive for Rational Mechanics and Analysis*, Vol. 72, 1979, pp. 99-140.

3 Chater, E., Hutchinson, J. W., and Neale, K. W., "Buckle Propagation on a Beam on a Nonlinear Elastic Foundation," to appear in a *Proceedings of the IUTAM Symposium on Collapse*, University College, London, Aug. 1982.

4 Hutchinson, J. W., and Neale, K. W., "Neck Propagation," to be published in *Journal of Mechanics and Physics of Solids*.

5 Ogden, R. W., "Elastic Deformations of Rubberlike Solids," in *Mechanics of Solids, The Rodney Hill 60th Anniversary Volume*, Hopkins, H. G., and Sewell, M. J., eds., Pergamon Press, 1982, pp. 499-538.

6 Palmer, A. C., and Martin, J. H., "Buckle Propagation in Submarine Pipelines," *Nature*, Vol. 254, 1975, pp. 46-48.

7 Mesloh, R., Johns, T. G., and Sorenson, J. E., "The Propagating Buckle," *Proceedings BOSS 76*, Vol. 1, 1976, pp. 787-797.

8 Kyriakides, S., "The Propagating Buckle and its Arrest," Ph.D. Thesis, California Institute of Technology, Pasadena, Calif., 1980.

9 Kyriakides, S., and Babcock, C. D., "Experimental Determination of the Propagation Pressure of Circular Pipes," ASME *Journal of Pressure Vessel Technology*, Vol. 103, 1981, pp. 328-336.

10 Kyriakides, S., and Babcock, C. D., "Large Deflection Collapse Analysis of an Inelastic Inextensional Ring under External Pressure," *International Journal of Solids and Structures*, Vol. 17, 1981, pp. 981-993.

11 Kyriakides, S., and Arikan, E., "Post-Buckling Behavior of Inelastic Inextensional Rings Under External Pressure," ASME JOURNAL OF APPLIED MECHANICS, Vol. 50, 1983, pp. 537-543.

APPENDIX

Numerical Scheme for Ring Analysis

The method used to generate the relation $p(\Delta A)$ shown in Fig. 7 is similar in many respects to the method employed in [10]. In the present study, for convenience, we did not enforce inextensionality, although the extensionality is not expected to have much effect on p^*. Furthermore, we constrained the ring

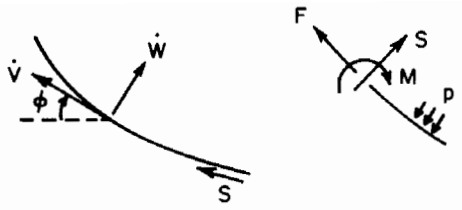

Fig. 11 Sign conventions for the ring analysis

deformations to be plane strain with zero axial component of strain, consistent with the fact that the ring segment is part of a long cylindrical shell.

The equilibrium equations for a ring in the deformed state are

$$\begin{aligned} dM/ds + S &= 0 \\ dS/ds - \kappa F &= p \\ dF/ds + \kappa S &= 0 \end{aligned} \tag{16}$$

where M, S, and F are the moment, resultant transverse shear stress, and resultant stretching stress with the sign conventions shown in Fig. 11. The curvature in the current state is $\kappa(s)$ and the distance along the ring midsurface is s. With $\dot{w}$ and $\dot{v}$ as the displacement increments normal and tangent, respectively, to the current middle surface, the increments of rotation, strain and curvature are

$$\begin{aligned} \dot{\phi} &= d\dot{w}/ds - \kappa\dot{v} \\ \dot{\epsilon} &= d\dot{v}/ds + \kappa\dot{w} \\ \dot{\kappa} &= d\dot{\phi}/ds \end{aligned} \tag{17}$$

With s_{ij} as the stress deviator, $\sigma_e = (3s_{ij}s_{ij}/2)^{1/2}$ as the effective stress, and $E_s(\sigma_e)$ as the secant modulus of the uniaxial stress-strain curve, the deformation theory relation for multiaxial stress states is

$$\epsilon_{ij} = \frac{1+\nu}{E}s_{ij} + \frac{1-2\nu}{E}\sigma_{pp}\delta_{ij} + \frac{3}{2}\left(\frac{1}{E_s} - \frac{1}{E}\right)s_{ij} \tag{18}$$

Let ϵ_{22} be the hoop strain and ϵ_{11} be the axial component of strain, with σ_{33} as the stress component in the direction normal to the middle surface. Under the conditions that $\sigma_{33}=0$ and $\epsilon_{11}=0$, one can derive an incremental expression from (18) relating $\dot{\epsilon} \equiv \dot{\epsilon}_{22}$ to $\dot{\sigma} \equiv \dot{\sigma}_{22}$ in the form $\dot{\sigma} = \bar{E}_t\dot{\epsilon}$, where $\bar{E}_t$ is the plane-strain tangential modulus which depends on the stress at the particular point in the ring. The incremental form of the constitutive relation for the ring is

$$\begin{aligned} \dot{F} &= L_1\dot{\epsilon} + L_2\dot{\kappa} \\ \dot{M} &= L_2\dot{\epsilon} + L_3\dot{\kappa} \end{aligned} \tag{19}$$

Here,

$$L_i = \int_{-t/2}^{t/2} \bar{E}_t z^{i-1}\,dz$$

with z as the coordinate measured from the ring middle surface.

After writing the equilibrium equations (16) in incremental form, we obtained four first-order differential equations with $\dot{S}$, $\dot{\phi}$, $\dot{\epsilon}$, and $\dot{\kappa}$ as dependent variables. This is a convenient choice of variables since $\dot{S}$ and $\dot{\phi}$ vanish at the quarter symmetry points. At each stage of the deformation history, the system of four first-order equations was integrated numerically. Then, the displacement increments were obtained by integrating the first two equations of (17) subject to $\dot{v}=0$ at quarter symmetry points. The increment in area reduction is $-\int\dot{w}ds$. An accurate evaluation of the integral on the right-hand side of (13) was obtained by fitting the discretized results for $p(\Delta A)$ using cubic splines.

Printed in U.S.A.